University of Iowa

Iowa Research Online

Theses and Dissertations

Fall 2012

Localization of vibration-based damage detection method in structural applications

Charles Joseph Schallhorn
University of Iowa

Recommended Citation

Schallhorn, Charles Joseph. "Localization of vibration-based damage detection method in structural applications." MS (Master of Science) thesis, University of Iowa, 2012.
https://doi.org/10.17077/etd.n1ptb50n

LOCALIZATION OF VIBRATION-BASED DAMAGE

DETECTION METHOD IN STRUCTURAL APPLICATIONS

by

Charles Joseph Schallhorn

A thesis submitted in partial fulfillment
of the requirements for the Master of
Science degree in Civil and Environmental Engineering
in the Graduate College of
The University of Iowa

December 2012

Thesis Supervisor: Associate Professor Salam Rahmatalla

Graduate College
The University of Iowa
Iowa City, Iowa

CERTIFICATE OF APPROVAL

_____

MASTER'S THESIS

_____

This is to certify that the Master's thesis of

Charles Joseph Schallhorn

has been approved by the Examining Committee
for the thesis requirement for the Master of Science
degree in Civil and Environmental Engineering at the December 2012
graduation.

Thesis Committee: _____
               Salam Rahmatalla, Thesis Supervisor

              _____
               Jasbir Arora

              _____
               Thanos Papanicolaou

ACKNOWLEDGMENTS

ABSTRACT

Vibration-based damage detection methods are used in structural applications to identify the global dynamic response of the system. The purpose of the work presented is to exhibit a vibration-based damage detection algorithm that localizes the sensor arrangements such that irregularities within the structural system can be detected, located, and quantified. Damage can occur in a structure either within the material or at a connection between segments; therefore two different types of specimens, a plate specimen and a connection specimen, were analyzed with the algorithm. Numerical and experimental analyses were completed for each of the specimen types, and the results prove that damage can be detected, located and quantified in each scenario. It is noted that the quantification of the damage is based on a supervised learning method (original and damaged states are known) and that the accuracy in which the damage is quantified within the scope of this work might have difficulty in unsupervised learning methods (only current state is known). This work will extend to be applied on a highway bridge as a basis for a structural health monitoring system, as preliminary results suggest that further refinement is needed.

TABLE OF CONTENTS

LIST OF FIGURES

INTRODUCTION

Damage detection and structural health monitoring (SHM) have become vastly popular within the field of structural engineering over the past few decades. These methods and procedures are utilized in order to characterize the structural integrity of a system and to provide a decision whether or not the system has the appropriate bearing capacity. Damage detection methods can be classified as destructive or non-destructive. Non-destructive methods are preferred over destructive methods such that the system could remain in function during and after testing. Of the non-destructive damage detection methods, both static-based and vibration-based methods are used to effectively determine static and dynamic responses of the system, respectively.

The dynamic response of a structure is described as the influence or motion of the system due to a non-static loading, such as an impulse load or forced vibration. Generally, the dynamic response is a measure of the vibration of the system. Equations of motion have been commonly used to solve for the displacements, velocities and accelerations at determined locations, thus resulting in the motion of a system due to an applied force. These equations of motion are shown in Equation 1, where $[M]$ is the mass matrix of the system, $[C]$ is the damping matrix, $[K]$ is the stiffness matrix, $\{\ddot{u}\}$ is the nodal acceleration vector, $\{\dot{u}\}$ is the nodal velocity vector, $\{u\}$ is the nodal displacement vector, and $\{F^a\}$ is the applied force vector.

$$[M]\{\ddot{u}\} + [C]\{\dot{u}\} + [K]\{u\} = \{F^a\} \tag{1}$$

In theory, the mass, damping and stiffness matrices as well as the applied force vector are all known quantities, therefore Equation 1 is used to solve for the nodal displacements and their time derivatives. Once these values are determined, the

acceleration can be transformed from the time domain to the frequency domain by applying a Fourier transform. Changes in the response of the system can be seen in the time domain, however, they can be seen more easily in the frequency domain as changes in the modal parameters (natural frequencies and mode shapes) of the system. The natural frequency of a structure is a frequency in which energy is trapped in the system. When the applied loading matches the natural frequency of the structure, the results are large deformations and possible failure. The natural frequencies of a system are determined by using Equation 2.

$$\omega_n = \sqrt{\frac{[K]}{[M]}} \tag{2}$$

As shown, the natural frequencies of the system are directly related to the mass and stiffness of the structure. Damage is categorized as a reduction in functionality of a system, which is usually a resultant of a reduction of mass or stiffness. Therefore, a change in the natural frequency of a system can be interpreted as damage being introduced into that system.

For the purposes of clarity, damage is defined for the scope of this work as any change in the structural integrity of a system. The most prominent feature that engineers are concerned with is any damage that is considered to be a reduction of functionality of the system. In structural engineering, a reduction of functionality generally suggests a loss of load carrying capacity or lack of control under dynamic loading. With this understanding of damage, changes in structural properties of the system can be acquired in order to detect damage states in a system.

Another technique to determine the response of a system using the frequency domain is to calculate the frequency response function (FRF) of the system. The FRF, also called the transfer function, is a ratio of any input signal to that of any output signal. It is common that the FRF is calculated with displacement or acceleration as the output and force as the input, but could also be calculated with displacement or acceleration as both the input and output signals by using reference and response sensors. The equation used to determine the frequency response function for an applied force input signal and a displacement output signal is shown by Equation 3.

$$\frac{X(\omega)}{F(\omega)} = \left(\frac{1}{[K]}\right)\left(\frac{\omega_n^2}{\sqrt{(\omega_n^2-\omega^2)^2 + (2\,\xi\,\omega\,\omega_n)^2}}\right) \tag{3}$$

With this transfer function, a graph is obtained. Peaks on this graph are considered to be locations of natural frequencies. If the natural frequency of the system were to decrease, as predicted with the implementation of damage, these peaks would decrease in magnitude and in frequency, thus shifts in these peaks down and to the left would be indication that damage is present. For this reason, the FRF of a structure can be used as a damage detection indicator.

In many applications, however, it is common that the applied force vector which can be measured is the only known quantity and it is also common that all of the information about the mass, stiffness and loading of the structure is unknown. In order to calculate the response of the system in these applications, sensors are used to gather acceleration data (displacement and velocity data may also be used) directly from any loading scenario desired on the structure. If the force is known, the FRF can then be determined as the ratio between the output acceleration and the input force using the same process as described previously.

If the applied force is unknown, which is usually the case for most structures outside of the laboratory, a different approach is needed to determine the FRF. Operational modal analysis is the process in which operational forces such as traffic and wind loads are used to excite the system, while the response is measured at different locations. In order to calculate the FRF in an operational modal analysis, a single reference location is chosen and all other locations are considered to be responses. The FRF is then calculated by the ratio of the response signal over the reference signal. This FRF shows the differences between the reference and the response signal, and changes to this function correspond to a change in relationship between the reference and response signal. If no damage is present in a structure and the sensors are located in close proximity with each other, the motion response of the structure will behave similarly, therefore the FRF will be expected to be close to zero. If damage is present in a structure not between the sensors, the motion response of the structure is expected to behave similarly to that of the non-damaged scenario. If damage is present in a structure between the sensors, the motion response of the structure is expected to behave differently than that of the non-damaged scenario, in such a manner that the magnitude of FRF decreases with damage.

These frequency analysis procedures are the basis for the numerical and experimental analyses completed in this work. With the process of collecting and analyzing data for these analyses understood, the types of specimens to investigate must also be considered. Damage can occur within the material of a structure or at the connection of different segments, therefore two specimens were examined for the scope of this work. A plate specimen with a groove successively deepened at a location

perpendicular to the length of the plate represents damage occurring within the material of a structure. A connection specimen in which bolts are successively removed from the joint represents damage occurring at the connection of two segments. These two specimens were used to validate the algorithm described in this work both numerically and experimentally.

It would be possible to adapt this method to numerous types of structures. Detection methods current in practice are used on structures such as bridges, airplanes, and motors, amongst many others. The purpose of this work is to devise a method that could be implemented onto similar structures and efficiently and accurately detect damage within the system with which it is implemented on. The end goal of this work is to expand the algorithm presented to be applied on a highway bridge. The justification for this goal is that the damage detection algorithm could be used as a basis for a structural health monitoring system with the capabilities to detect, locate and quantify any irregularities within the structure.

Vibration-based damage detection generally consists of a number of sensors placed on a system such that a global response can be measured by using the previously described analysis procedures. Damage is detected by noting any change in this global response when comparing it to a response gathered at a previous time period. It is proposed that by arranging the sensors in such a manner to replicate local damage detection, i.e. increase the number of sensors or arrange the sensors in specified locations and orientations, that damage could be detected, located, and quantified.

CHAPTER 1. LITERATURE REVIEW

Infrastructure health conditions and monitoring have attracted public attention and have been an active area of research and development for the last several decades. This is due to the urgent demands for safer and longer life structures and in response to sudden catastrophic failures. Many novel ideas have been developed and implemented toward achieving the goals of checking the integrity of the structures to deal with the four levels of damage assessment, summarized by (Rytter 1993) as existence of damage, localization of damage, extent of damage, and prediction of the remaining loading capacity of the structure. In theory, most of these ideas have shown noticeable success using simulations, but have difficulties in detecting damages on large structures. This could be attributed to the complexity of these structures (Li and Wu 2007) and the limited ability of the current sensors in detecting damage in the presence of noise and environmental effects/interferences. Advances in nanotechnology and biosensing have pushed the research in the area of sensing and actuating to new frontiers and have led to the introduction of many smart and novel sensors with multi-functionality. These new sensors will open the door for many opportunities toward affordable and effective structural health monitoring systems.

Structural health monitoring methodologies can be classified as global and local schemes. Global methods based on the changes in dynamic responses of structures have shown good potential in detecting the first three levels of damage specified by(Rytter 1993). These methods have been under investigation for several decades, and many ideas and algorithms have been developed, tested, and implemented using computer simulation, lab testing, and real-sites testing (Pandey, Biswas et al. 1991; Rytter 1993;

Farrar and Jauregui 1998; Sampaio, Maia et al. 1999; Wahab and Roeck 1999; Duffey, Doebling et al. 2001; Maia, Silva et al. 2003; Humar, Bagchi et al. 2006; Li and Wu 2007; Cruz and Salgado 2008; Adewuyi, Wu et al. 2009).

Local methods include traditional strain gauges, fiber optics, tap testing, MEMS devices, acoustic approaches, X-rays and Gamma rays, and radar technology(Chase 2001). These sensors can be very effective; however, each sensor can give only partial information about the health situation of the structures, not the whole status. (Chang, Flatau et al. 2003) discussed the benefit of the tap test in spite of being time consuming. They also highlighted the advantages of the wireless sensors in minimizing the cost and noise of the wire systems.

Many methods have been derived to possibly achieve an effective manner in which to accurately sense damage in a system without first knowing the structural integrity of the model or by performing invasive procedures. In order to accurately incorporate any detection method with any already existing system, an unsupervised learning mode would most likely be needed to be successfully implemented. This unsupervised learning mode describes the lack of information from a previous healthy state of the model, such that the damage detection is directed toward any statistical differences found in damage sensitive features, determined by recognizing patterns or changes in structural responses such as natural frequency, mode shape, or damping ratios (Cruz and Salgado 2008). The change in the damage sensitive features is developed from the assumptions that any change in the response of the system is a result of a change in its structural properties, mainly stiffness and mass. The change in stiffness directly relates to a change in natural frequency in the model, therefore damage can be detected by

characterizing the changes in the frequency response function (FRF) that correlates the system response and the input excitation.

By using this process, many damage detection methods have been created in order to attempt to portray deficiencies within a structure. (Cruz and Salgado 2008) describe in detail a few of the vibration-based damage detection methods in the field currently, as well as quantitatively describe each of these methods by applying them to both simulated vibration data and data gathered from damage testing on the Övik Bridge in Sweden. The methods described by Cruz and Salgado are the coordinate modal assurance criterion (COMAC) method, the curvature method, the damage index (DI) method, and the wavelet analysis method. The COMAC method is a simplistic correlation of the mode shapes and can produce accurate results for severe damage. The curvature method states that the mode shape curvature is related to the flexibility of the structure and produces accurate results for severe damage and smooth mode shapes. The DI method relates to the strain energy in a beam during deformation, and is dependent on the mode shape curvature, therefore produces results with similar accuracy to that of the curvature method. The wavelet analysis method allows for an analysis of the measured data with variable size windows, which allow for the detection of damage to occur without the loss of data by Fourier Transforms. (Yang et al. 2004) discuss in an article that the Hilbert-Huang based approach is "capable of decomposing a signal… more precisely than the wavelet analysis [method]". The Hilbert-Huang method is the process in which to determine the time in which damage occurs, separate the data into segments of before damage and after damage, then compare damage sensitive features from each segment of data. The conclusions based on this method state that the analysis is not sensitive to

noise, can accurately calculate the damage sensitive features for before and after the damage, and is accurate in locating the damage for both sudden stiffness loss and gradual stiffness changes in the structure.

Sensitivity to noise, albeit a large factor in consideration with damage detection methods, is just one of the components that must be accounted for. (Peeters et al. 2001) discuss the effect that temperature has on vibration-based damage detection by means of creating confidence intervals from data gathered for an undamaged structure that are used as baseline regions for future readings. If a measurement lies outside of the given confidence interval, the structure would be considered damaged.   Also described in the article by (Peeters et al. 2001) is the effect of the input excitation on the damage detection process. To test these effects, data collection for different excitation procedures were conducted, such as ambient excitation (wind, traffic, etc.), shakers, and drop weights. The conclusions from these scenarios state that the shakers were expensive and resulted in similar findings as the ambient excitations, the ambient excitations could allow for continuous monitoring, while the drop weights allowed for inexpensive intermittent monitoring.

The obvious theme of this work is to show that vibration-based damage detection approaches are heavily investigated as global methods; however, they have not been approached as local damage detection schemes. The goal of this work is to use vibration-based damage detection approaches as local methods to quantify damage at critical areas in structures.

Upon reviewing these articles on damage detection methods, a few considerations were noted that would supplement the author's investigation of a refinement to or a

creation of a vibration-based damage detection method. These considerations include: 1) Which damage sensitive parameter(s) should be considered; 2) In order to accommodate a broader scope, the unsupervised learning process should be taken into account; 3) What sensitivity does the method have with regards to noise, damage severity, temperature, etc.; 4) How can the detection system provide accurate damage prediction or notification after implementation. These considerations could increase the potential for a damage detection method that would be desirable for practical applications.

CHAPTER 2. DAMAGE DETECTION ALGORITHM

An algorithm was created for the use of detecting damage in a system by localizing acceleration sensors. This algorithm is outlined in Figure 1. Although the individual aspects of this approach are fairly well established, it is noted that the application of this process to be utilized for dynamic damage detection is unique when localizing the sensors such that damage can be detected, located and quantified.

- Gather acceleration data from a system or model
- Process/Filter data to obtain FRF for each sample
- Determine regions of high coherence/strong correlation
- Compare FRF for damage scenarios at said regions
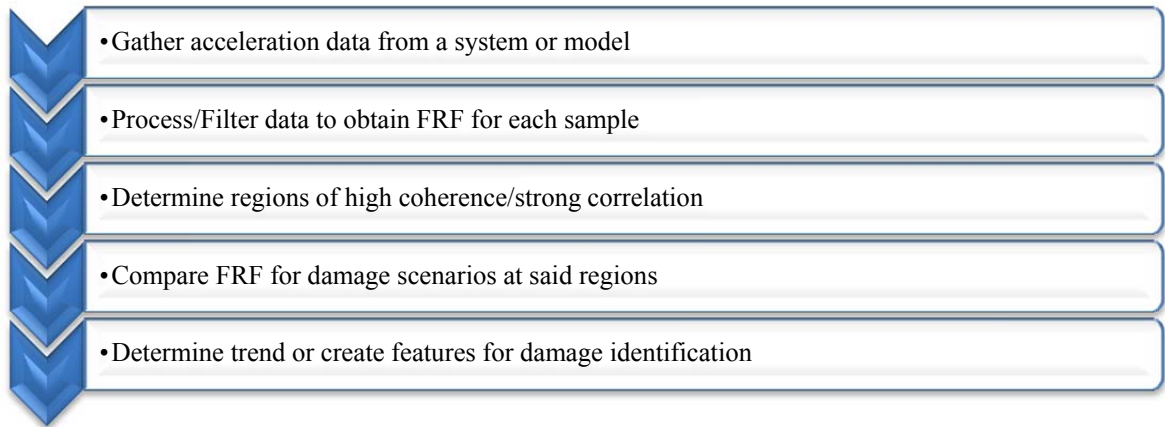- Determine trend or create features for damage identification

Figure 1. Outline of Damage Detection Algorithm

Before initiating the algorithm, the types of specimens and the loading scenarios were established such that the algorithm could best incorporate a multitude of damage scenarios. As stated previously, damage can occur within the material of a structure or at the connection of different segments, therefore two specimens were examined for the scope of this work. A plate specimen with a groove successively deepened at a location perpendicular to the length of the plate represents damage occurring within the material of a structure. A connection specimen in which bolts are successively removed from the

joint represents damage occurring at the connection of two segments. These two specimens cover the basic concepts behind a majority of the damage scenarios that could occur within a real structure.

Transient analyses were simulated for all of the specimens in this work, with the exception of a harmonic analysis that was completed for the finite element model of the connection specimen. A transient analysis is used to determine the free-vibration response of a system due to an impact loading scenario. The definition of an impact loading scenario is that any load is applied to the system for a short time duration. The purpose of a transient analysis is to measure the response of a structure during and after the impact, thus giving the response of the free-vibration of the system where no loading is applied. This is useful because one could investigate how the energy inputted into the system by the impact travels throughout the structure. Also, the FRF calculated by the acceleration or displacement due to the impact allows one to understand the frequency ranges in which damage is most likely to occur in. For the harmonic analysis completed for the connection specimen, the loading was not considered as an impact, but rather a sinusoidal load, thus resulting in the response being a forced-vibration, rather than free-vibration. This type of analysis gives rise to a similar understanding of the frequency ranges in which damage is more likely to occur, with the exception that the harmonic analysis has frequency components that tend to mimic those of the loading frequencies. With this understanding, the transient analysis was chosen for the majority of the specimen examinations.

With this approach and for the specified analyses, acceleration data was collected for a real structure or simulation by localizing accelerometers around the area of interest.

This area of interest was the position where damage was most likely to occur; therefore the dynamics of the system was well enough understood such that the orientation of the principle directions of motion was known and thus the direction in which damage had the greatest probability to develop. One sensor, further noted as the reference sensor, was located away from this area but at a location of high motion such that a well-defined signal was present for the reference sensor. The signal from the reference sensor is important when calculating the FRF of the system due to the procedure in which the operation modal analysis is conducted. As previously described, the FRF for an operational modal analysis can be calculated by taking to the ratio of the response at any location on the system to the response at the reference location. The multiple response locations can be considered to be "normalized" by the reference signal. The justification for the reference sensor being away from the influenced area is that the accuracy of detecting damage by a sensor is related to the proximity of the sensor to the damage. The motion captured by the response sensors should be more affected by the damage than the motion captured by the reference sensor in order to obtain clear results.

Also to obtain better results, and if it was permitted, acceleration data from multiple impacts was collected. Otherwise, a single impact was used for the analysis. Using data from multiple impacts is preferred because this would allow one to see the consistency of the data being collected and would give statistical significance whether or not the data gathered was accurate. The data was then filtered with a band filter to investigate a range of frequencies in order to detect damage. The high pass filter was used to remove the noise caused by the DC component of the sensor. This filter removed any frequency component that was related to 10 Hz or less. A low pass filter was also

applied due to the understanding that the structures being analyzed generally had low
natural frequencies, thus higher frequencies were not required to capture the dominant
mode shapes. This filter removed the components higher than 100 Hz. Processing the
data included cutting each impact sample in the time domain such that only the impact
and the response are looked at and then storing these impact samples collectively for each
damage scenario. The FRF was calculated from these processed data sets using Equation
4 and then averaged to output a single FRF for each of the damage scenarios.

$$FRF\ (dB) =\ 20\ log_{10}\left(\frac{Response\ Signal}{Reference\ Signal}\right) \tag{4}$$

The purpose for using this equation to calculate the FRF is such that the logarithmic scale
clearly identifies all frequency components that the signal is composed of. When looking
at the same signal with a linear scale, only the frequency components with maximum
magnitude are visible, thus the logarithmic scale exaggerates the magnitude but clearly
depicts the majority of frequency components.

Characterizing the FRFs for each damage scenario before averaging allows for the
regions of strong correlation to be obtained by noting where the FRFs are "tight", i.e.
minimal variation between each impact sample. This strong correlation defines the
ranges in which the structure always responds in a similar manner, thus these ranges are
where the most accurate results appear. When available, the regions of high coherence
were also calculated to determine frequency ranges where the signals were considered
linear. The coherence is a statistical process in which to measure the relationship
between two signals in a linear system. Coherence is calculated by using Equation 5,
where G_{xy} is the cross-spectral density between signals x and y, and G_{xx} and G_{yy} are the
auto-spectral densities for signals x and y, respectively. The values obtained by this
calculation are used to determine ranges in frequency in which noise or nonlinearity
occurs between the signals.

$$C_{xy} = \frac{|G_{xy}|^2}{G_{xx}G_{yy}} \tag{5}$$

One of the underlying assumptions with regards to structures and damage detection is that the system behaves linearly. If this assumption holds true, then only regions of linearity, i.e. regions of coherence close to a value of one, would ensure accurate results.

A comparison of the averaged FRFs for each damage scenario was then completed for the regions where the signals had high coherence or strong correlation. These regions are of importance due to the statistical variation in which the average FRF was calculated; the larger variation between impact samples could cause for inaccurate damage identification at that region. The optimal comparison would be between average FRFs for varying severity damage scenarios when each of the average FRFs have small standard deviations, thus resulting in a high accuracy in identifying the specific damage scenario. For regions of high coherence or strong correlation, the standard deviation between FRFs is usually low, thus ensuring fairly accurate results.

Upon completion of the comparison between the averaged FRFs, trends or patterns in the responses due to damage are determined by visual inspection or feature extraction. Based on the theory behind the modal analysis procedure, it is predicted that the expected trend that the FRFs should have would be that the magnitude of the FRF decreases for an increase in damage. If this predicted trend is not clearly visible, then feature extraction would be needed to determine how the response of a system behaves due to damage scenarios. Features for the response of a system could include, but is not limited to, taking the sum or average of the magnitudes of the FRF for a given frequency

window or windows. The trends or features could then be used as parameters for identification of a current damage state or a prediction of a future damage state.

The use of this algorithm for detecting damage by localizing dynamic sensors has a fairly simplistic approach, but requires an understanding of how the system should respond dynamically even before beginning the data collection process in order to ensure accurate results. Although the statistical parameters (correlation and coherence) assist in knowing the appropriate regions to investigate, knowing the orientation and placement for the localization of the sensors is how the algorithm becomes the most effective.

CHAPTER 3. PLATE SPECIMEN ANALYSIS

Finite Element Modeling of Plate Specimen

In order to prove the concept that by localizing accelerometers, damage could be detected and quantified, a finite element model was created for a simple plate specimen. The use of this finite element model would calculate the acceleration data without any noise and could be analyzed in order to determine damage detection features. These features could then be used as a basis for a decision whether or not the structure is damaged as well as a quantification and location of the damage.

The finite element model was constructed using the educational version of the commercial software ANSYS (ANSYS 2010). The plate specimen to be modeled is 28" long by 3" wide by ¼" thick and pin-pin supported at each end. The material properties used for the creation of the plate specimen were assumed to be standard A36 steel properties ($E = 29,000$ ksi, $\nu = 0.3$, $\rho = 0.291$ lb/in^3). Three PLANE182 (with thickness) segments were created in order to simulate the plate specimen and a crack section (Figure 2). The crack section is modeled by a thin variable stiffness plate segment in between two healthy plate segments. The variable stiffness plate segment is used to create different damage severities in the specimen by altering the material stiffness parameter of this segment; therefore no re-meshing is required between damage scenarios. Nodes 1, 2, and 3 are the nodes of interest for acceleration data to be gathered for, and Node 4 is the location of the impulse force.
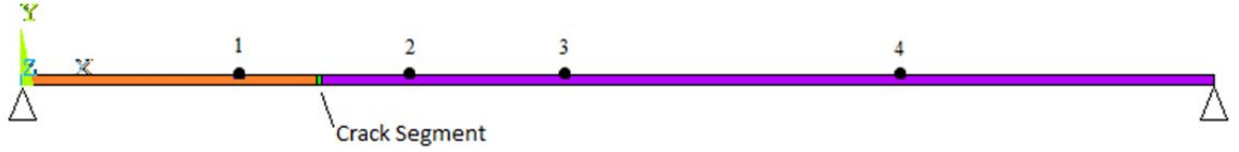
Figure 2. Finite element model of plate specimen showing the crack segment located between two healthy material segments and the location of nodes used for the completed analysis

A transient analysis was conducted on this specimen using ANSYS in order to determine the dynamic response of the system to an impulse load. General equations of motion were used to solve for the accelerations at the nodes of interest, as described previously. The equation of motion is shown again in Equation 6. From the input parameters above, the mass matrix is known by inputting the density, the damping matrix is known by inputting the Rayleigh damping coefficients (Equation 7), the stiffness matrix is known by inputting the modulus of elasticity (for both the cracked segment and the healthy segment), and the applied force is known by inputting the impulse force acting at node 4.

$$[M]\{\ddot{u}\} + [C]\{\dot{u}\} + [K]\{u\} = \{F^a\} \tag{6}$$

The calculation for the Rayleigh damping coefficients, α and β, was completed by using Equation 6. When applying an orthogonal transform to these matrices, i.e. uncoupling the equations of motion, Equation 6 can be simplified and reduced to Equation 8, where ξ is the modal damping ratio and ω is the natural frequency of the system.

$$[C] = \alpha [M] + \beta [K] \tag{7}$$

$$2 \xi_i \omega_i = \alpha + \beta \omega_i^2 \tag{8}$$

For structural problems, mass damping (α damping) is generally ignored. To look at a frequency range up to 100 Hz, β was assumed to be 0.02 for the purposes of this research.

$$\beta = \frac{2\,\xi_i}{\omega_i} \qquad (9)$$

Using the modal analysis procedure addressed previously, the FRF for the specimen can be calculated by using Equation 10. Since the applied force vector is known, the displacements were directly calculated and accelerations were derived from these displacements with respect to time.

$$\frac{X(\omega)}{F(\omega)} = \left(\frac{1}{[K]}\right)\left(\frac{\omega_n{}^2}{\sqrt{(\omega_n{}^2-\omega^2)^2+(2\,\xi\,\omega\,\omega_n)^2}}\right) \qquad (10)$$

It is shown by this relationship and by the definition of the natural frequency that components of the response of the system could be either proportional or inversely proportional to the stiffness of the structure. Further inspection proves that the components that are proportional to the stiffness, i.e. the natural frequency, have a greater effect on the system than those that are inversely proportional, therefore it is expected that a decrease in stiffness of the structure would decrease the magnitude of the frequency response.

Three load steps were used for the analysis in order to create a 100 lb impulse force acting in the vertical (Y) direction on node 4 (Figure 3). The Newmark method is used within ANSYS to solve the system of equations for the transient analysis. This method utilizes finite differences in time, known as time steps, to calculate displacements. In order to ensure an accurate result, the appropriate time step was calculated by using Equation 11, in which *f* is the highest mode frequency of interest.

Since the upper bound on the range of frequencies being inspected was 100 Hz, it was
calculated that a time step of 0.0005 seconds should be used.

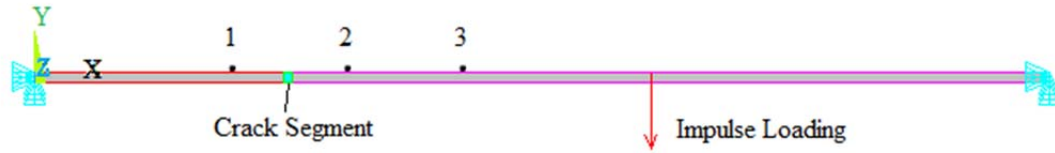$$\Delta t = \frac{1}{20f} \qquad (11)$$

Figure 3. Layout of the loading and boundary conditions for the finite element plate
specimen relative to the nodes used for the completed analysis

The solution was run and a time history of the displacement, and subsequently
acceleration, was calculated for varying damage severities (0%, 5%, 10%, 20%, 30%, and
40% reduction in stiffness). The notation used to distinguish these damage scenarios is
D#_Ref_Res, where # notes the percent reduction in stiffness, Ref refers to the reference
node, and Res refers to the response node. For example, D10_1_3 corresponds to the
damage scenario with 10% reduction in stiffness, with node 1 as the reference signal and
node 3 as the response signal. In order to model this reduction in stiffness, the material
property E for the crack segment only was changed to the appropriate percentage of
healthy stiffness, and the software analysis was rerun (Example: 10% reduction in
stiffness = 0.9 * 2.9x10^7 psi = 2.61x10^7 psi). The FRF from these damage scenarios
are shown in Figure 4.
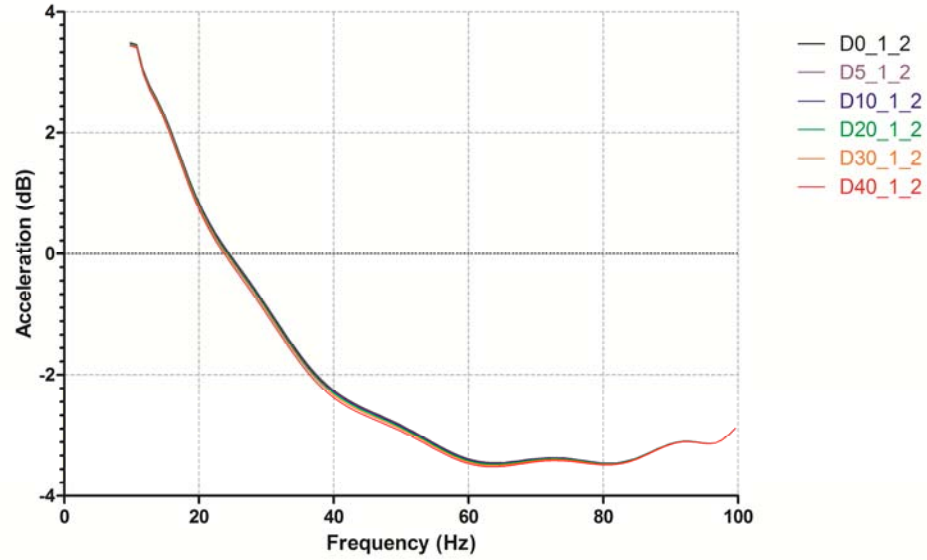
(a)
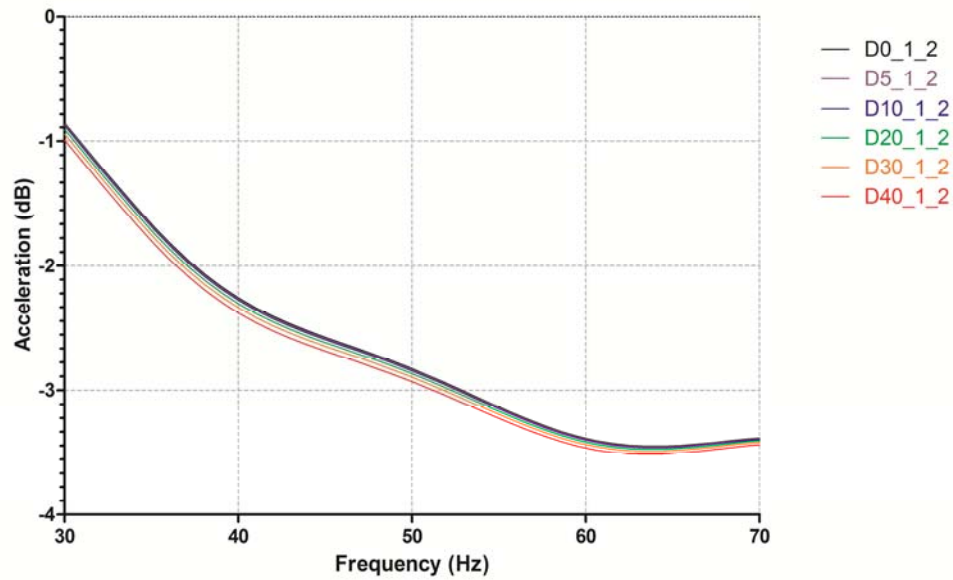
(b)

Figure 4. FRF Diagrams for plate specimen (a) Multiple damage scenarios for nodes 1 and 2 (b) Zoomed in portion showing the trend that damage creates in the response of the signals between nodes 1 and 2 (c) Multiple damage scenarios for nodes 1 and 3 (d) Zoomed in portion showing the trend that damage creates in the response of the signals between nodes 1 and 3 (e) Comparison showing the relationship between the responses of each pair of nodes
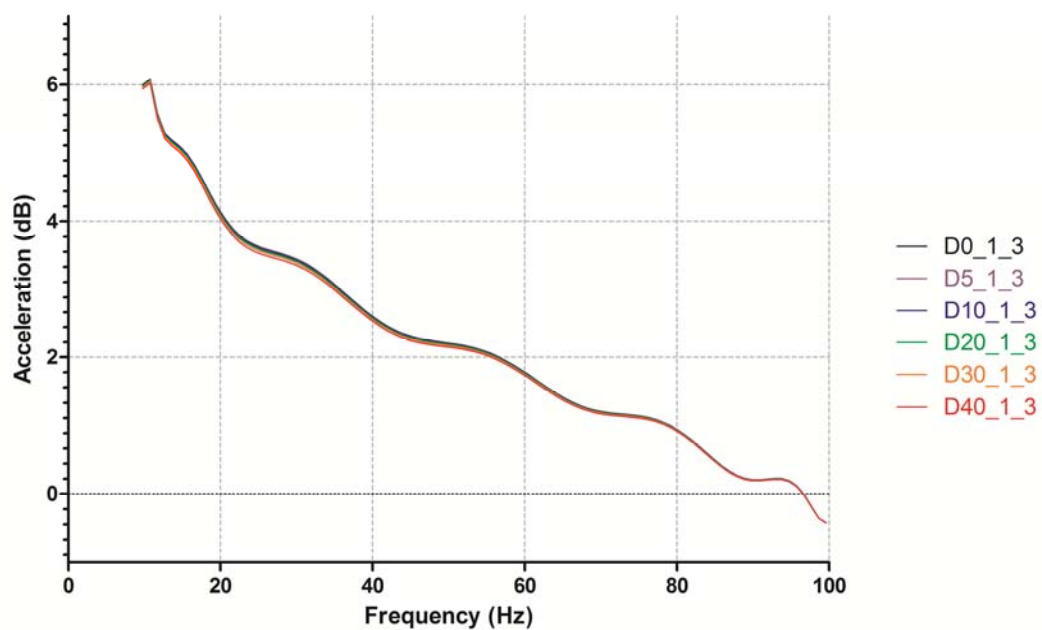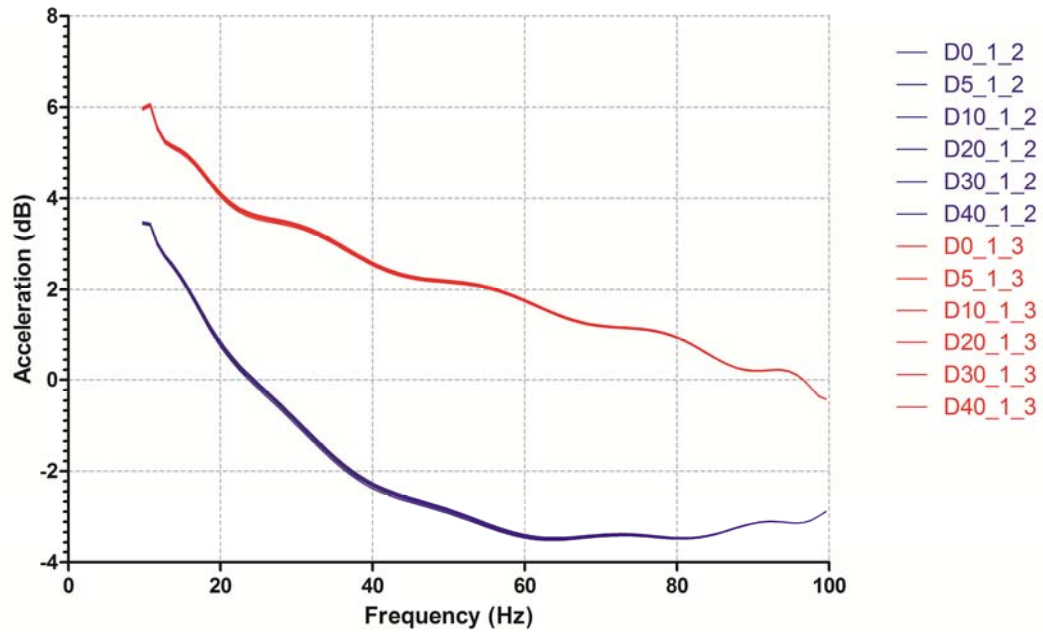
(c)
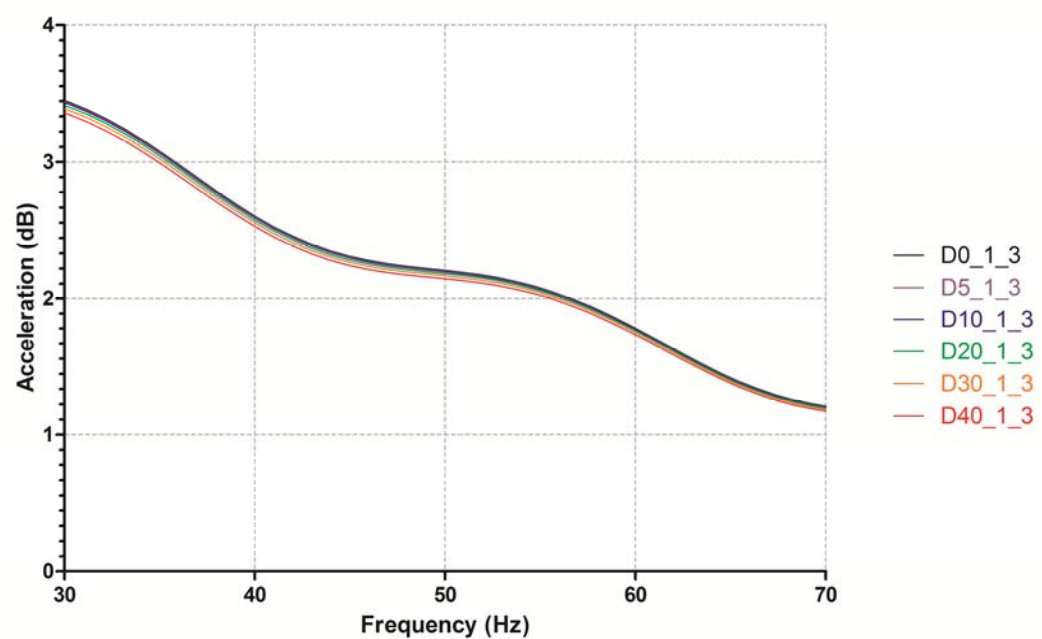
(d)

Figure 4. Continued

(e)

Figure 4. Continued

It is shown that damage scenarios can be identified and quantified for the plate segment. Visual inspection can faintly distinguish between healthy and damage scenarios but a closer look shows the trend that the FRF decreases and shifts to the left for each increase in damage. As predicted, for a decrease in stiffness, the natural frequency of the structure will decrease, hence the shift to the left, and the response of the system will decrease, hence the downward shift in magnitude. From this numerical analysis, damage can be found and quantified, although locating the damage was proven inconclusive.

Experimental Analysis for the Plate Specimen

An experiment was completed in order to validate the results from the finite element model. A geometrically similar plate was constructed and tested. The plate
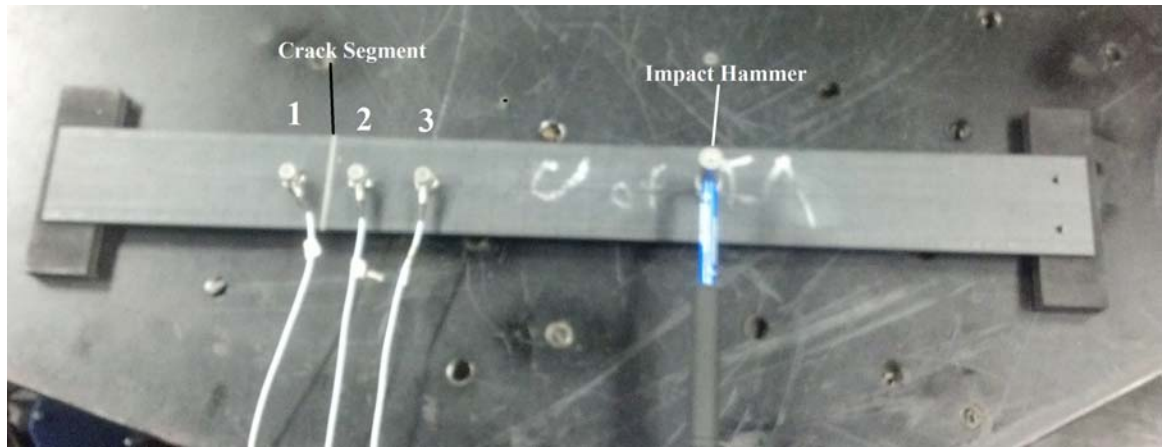
(a)
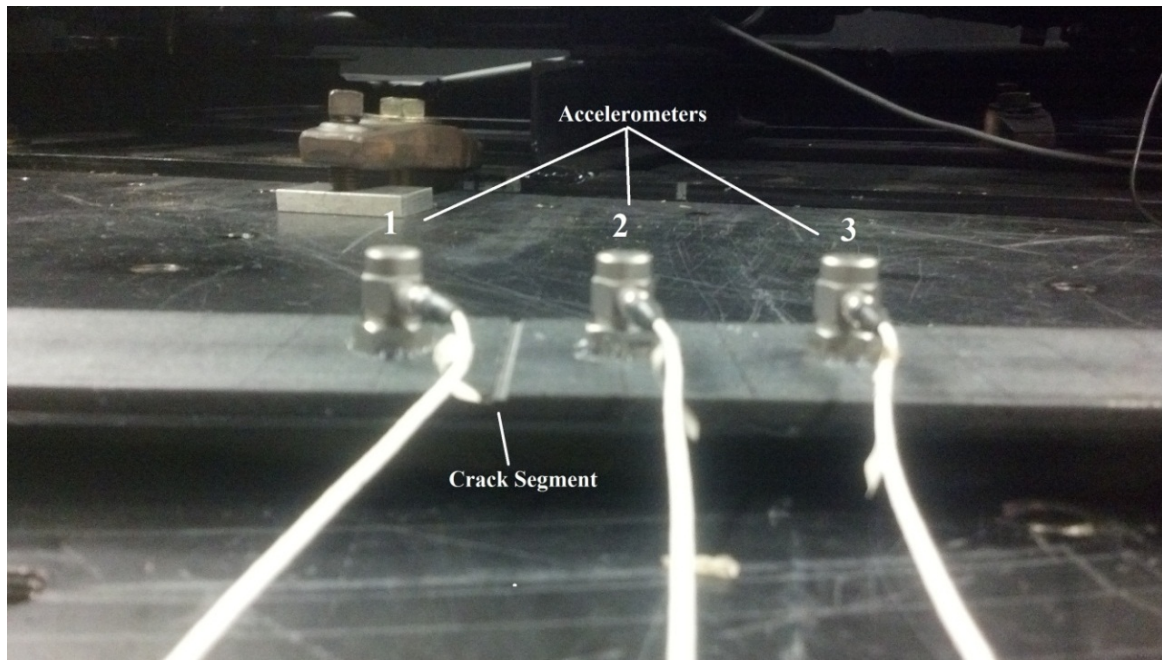
(b)

Figure 5. Experimental layout for plate specimen (a) Placement of the accelerometers, the location where the impact is loaded, and the support conditions at the ends of the plate (b) A close up view of the damage location and the sensors

specimen is 28" long by 3" wide by ¼" thick and supported on each end by a rubber pad. The material properties specified for the plate specimen were to be standard A36 steel properties (E = 29,000 ksi, ν = 0.3). Three accelerometers were placed each 2" apart from each other and an impact hammer was used to input an impulse force at a specified node. The layout of this experiment is shown in Figure 5. Acceleration data was gathered for all sensors for each of six damage scenarios (0%, 5%, 10%, 20%, 30% and 40% of thickness damaged). The damage was introduced by creating and successively deepening a groove in between sensors 1 and 2.

The data acquired for this experiment was then used to calculate the FRF for the plate specimen. The notation for each damage scenario is D#_Ref_Res, where # is the groove depth as a percentage of the overall thickness of the plate, Ref refers to the reference node, and Res refers to the response node. For example, D10_1_3 corresponds to the damage scenario with a groove removing 10% of the thickness of the plate, with node 1 as the reference signal and node 3 as the response signal. The averaged FRF of nodes 1, 2, and 3 for each damage scenario is shown in Figure 6.

<u>Plate Specimen Results and Discussion</u>

Similar to that of the finite element model of the plate specimen, it is shown that damage scenarios can be identified and quantified for the experimental plate segment. Visual inspection can distinguish between healthy (0% damage), moderate (5%, 10%, 20% and 30% damage) and severe (40% damage) damage scenarios. By analyzing the response for multiple impulses per damage state, each of the damage scenarios can be quantified by their respective damage percentage with high accuracy due to the strong correlation between samples. It is noted that the quantification of the damage can only be
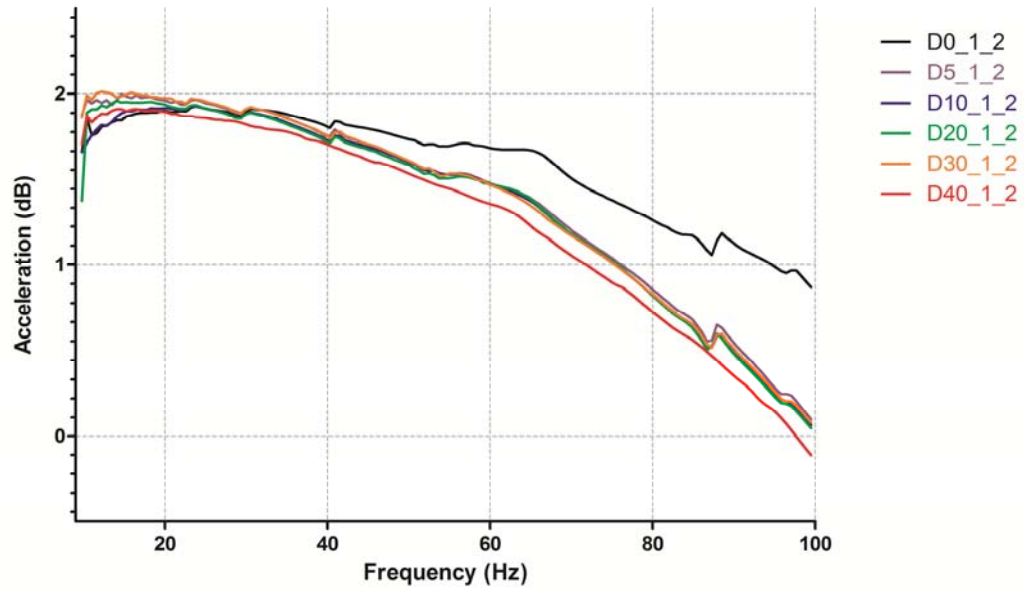
(a)
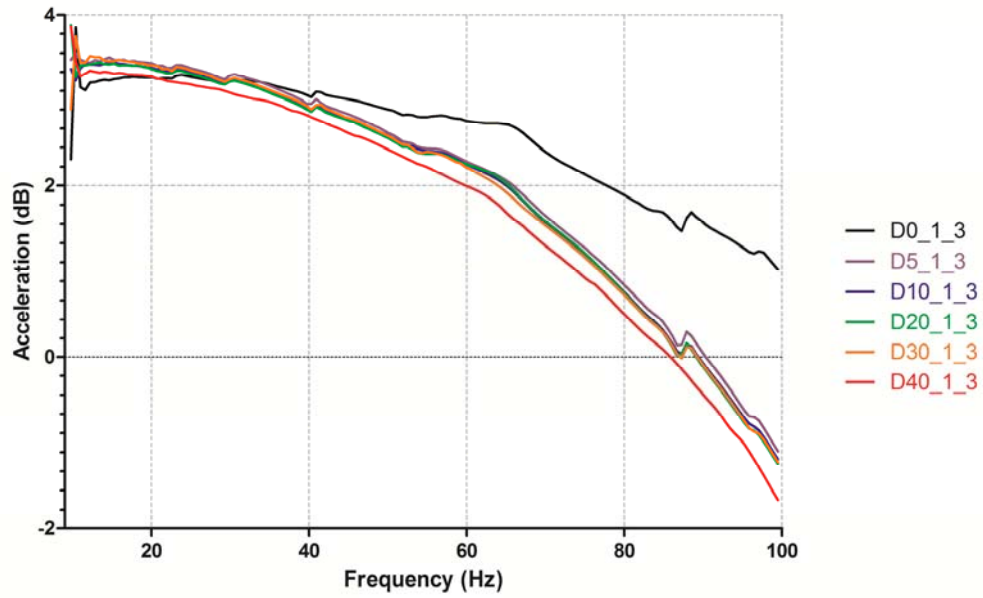
(b)

Figure 6. FRF diagrams for experimental plate specimen (a) Multiple damage scenarios for nodes 1 and 2 (b) Multiple damage scenarios for nodes 1 and 3 (c) Comparison between pairs of nodes showing that damage can be located by the larger variations between signals 1 and 3 than between signals 1 and 2
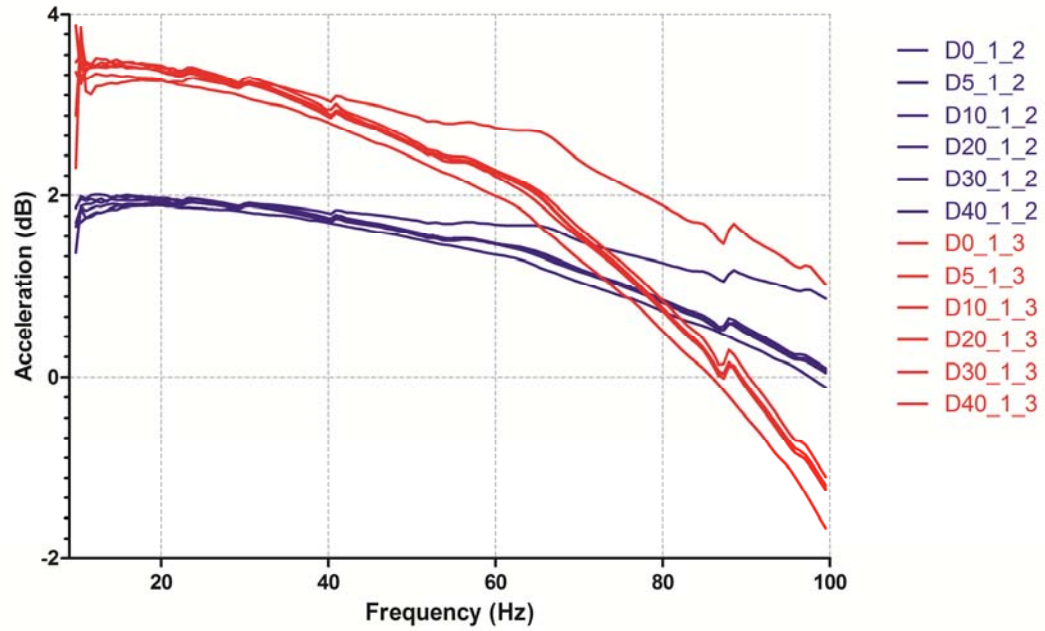
Figure 6. Continued

applied to systems in which a baseline or healthy scenario has be established, therefore

unsupervised learning methods must be quantified by changes in the response as viewed

from the initial inspection rather than as a percent damage.

The location of the damage can also be distinguished for the experimental plate

specimen when comparing the frequency response for two pairs of sensors using the

same sensor as a reference, i.e. comparing the FRF from reference sensor 1 response

sensor 2 to the FRF from reference sensor 1 response sensor 3. As shown in Figure 6c,

the changes in response to damage scenarios between sensors 1 and 2 are smaller than

those changes between sensors 1 and 3 for the same damage scenarios. This trend can be

explained by the interpretation that the sensor is affected by proximity to the damage.

The rate of change between damage scenarios for sensors 1 and 3 suggests that there is damage in the proximity of one of the sensors, although it is unknown which sensor the damage is nearest to. The rate of change between damage scenarios for sensors 1 and 2 also suggests that there is damage. The smaller rate of change between sensors 1 and 2 imply that damage is affecting sensors 1 and 2 more so than sensor 3, therefore damage is accurately located between sensors 1 and 2.

CHAPTER 4. CONNECTION SPECIMEN ANALYSIS

<u>Finite Element modeling for Connection Specimen</u>

A second finite element model was created in order to model a more realistic damage scenario represented by structural joints. The plate specimen of chapter 3 modeled a single continuous system, therefore the excitation, or energy, within this system was free to move anywhere within the structure. A more realistic approach would be to model a connection section that is comprised of multiple segments connected via bolts or welding at which the damage is located at the discontinuity of the material. The excitation within a connection specimen would be altered at these discontinuities, thus increasing the probability to accurately detect damage. A majority of failures in structures occur at connection locations; therefore an I-section was created to model symmetric tee connections. This specimen was designed to simulate the connection between two girders and a floor beam on a bridge. The model consists of five plates rigidly connected to each other, with two plates being bases for the specimen. It should be noted that the ANSYS simulation did not include bolt holes in any of the plate sections when compared to the experimental specimen shown in Figure 7. Instead, a thin variable stiffness plate segment was used at the connection locations, as shown in Figure 7b. Similar to that of the plate specimen, the variable stiffness plate segment is used to create damage in the specimen by altering the material stiffness parameter of this segment; therefore no re-meshing is required between damage scenarios. The material properties used for the creation of the connection specimen were assumed to be standard A36 steel properties (E = 29,000 ksi, ν = 0.3, ρ = 0.291 lb/in^3).
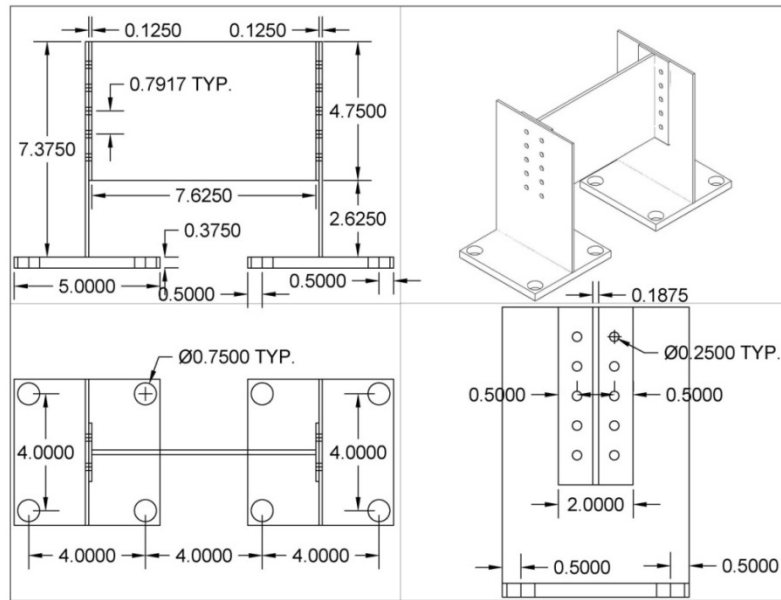
(a)
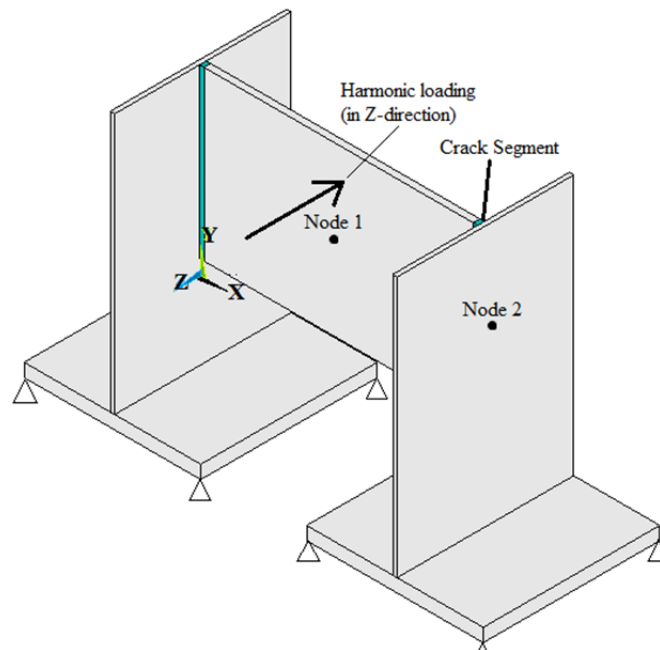
(b)

Figure 7. Design and layout of connection specimen (a) Connection specimen dimensions and layout (b) Finite element model showing the variable stiffness crack segment at the connection, loading direction, and boundary conditions

Before implementing the algorithm for this analysis, a preliminary numerical study was conducted to investigate the direction in which the FRF shows more sensitivity to the damage under consideration. This preliminary study was a harmonic analysis. This type of analysis is used to determine the response of system subjected to loads that vary harmonically (sinusoidal) with time. Results from this analysis were used to determine the FRF of the connection specimen for varying damage severities (0%, 10%, 20%, 30%, and 40% reduction in stiffness). The notation used to distinguish these damage scenarios is U*N-*-*D#, where the *N-** notes the axial direction and node number, and # refers to the percent reduction in stiffness. For example, UX-1-D20 corresponds to the X direction of node 1 with a damage scenario of 20% reduction in stiffness. In order to model this reduction in stiffness, the material property E for the crack segment of interest only was changed to the appropriate percentage of healthy stiffness, and the analysis was rerun (Example: 10% reduction in stiffness = 0.9 * 2.9x10^7 psi = 2.61x10^7 psi). The FRF from these damage scenarios are shown in Figure 8.

As shown by Figure 8, and referring to the coordinate system described in Figure 7b, the x-direction is the most affected by damage, which is noted by the amount of change in the FRF due to damage in this direction when compared to the other directions. This result is acceptable by understanding the dynamic motion of the structure throughout different damage scenarios. The damage being applied is in a plane perpendicular to the x-direction; therefore the change in motion between nodes 1 and 2 is maximum in this direction as damage increases. With this understanding, the x-direction was taken as the primary axis of interest for the experimental analysis of the specimen.
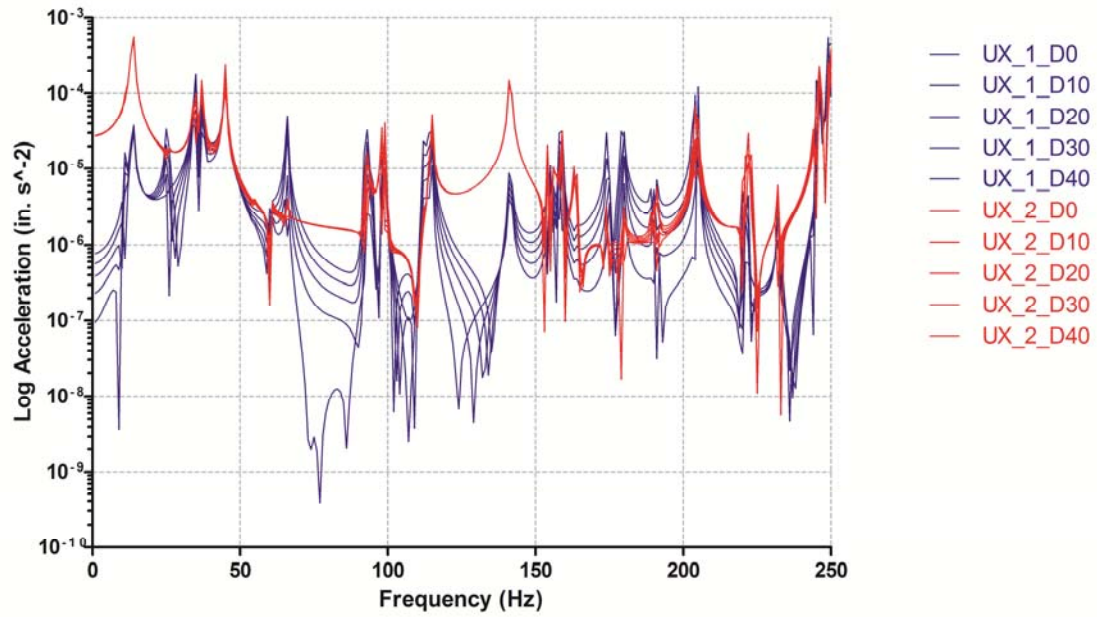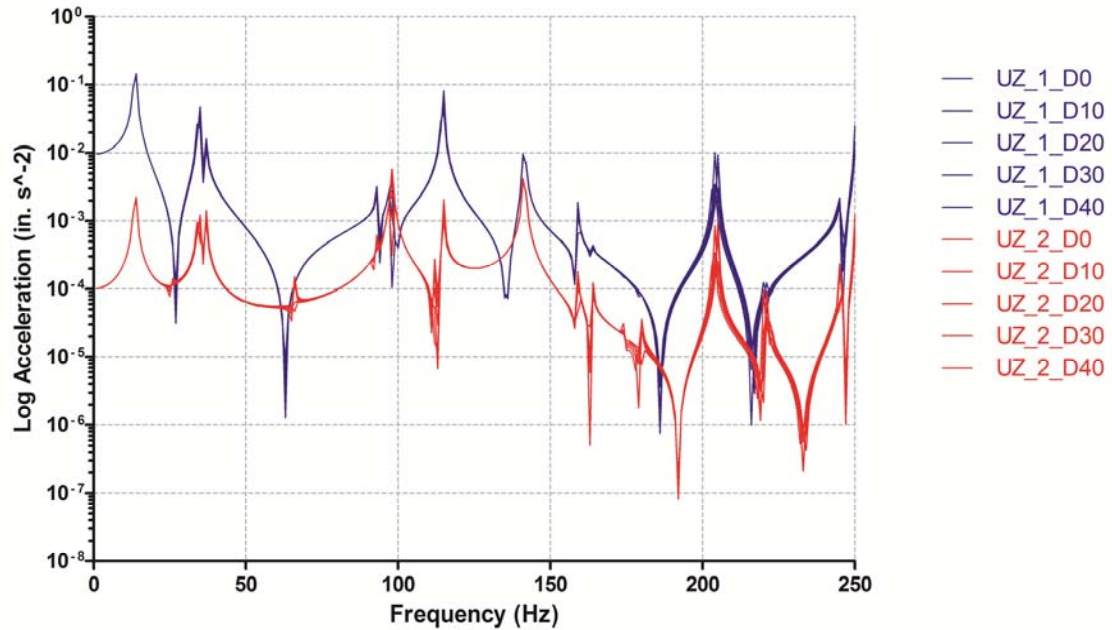
(a)
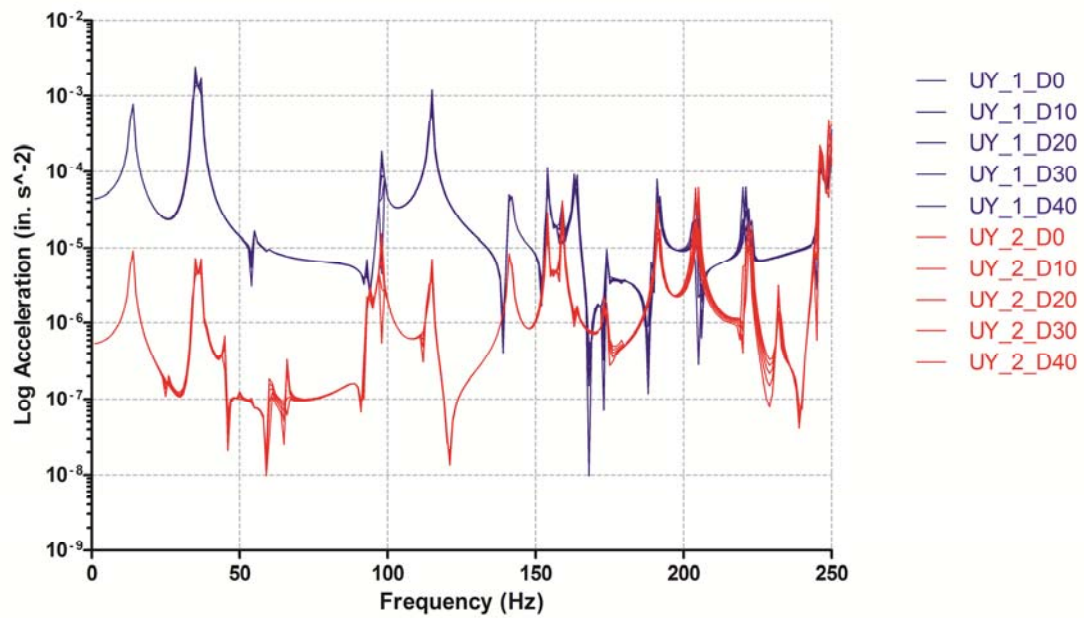
(b)

Figure 8. Harmonic response for nodes 1 and 2 of connection specimen (a) Response in the X-direction (b) Response in the Y-direction (c) Response in the Z-direction

(c)

Figure 8. Continued

Experimental Analysis for the Connection Specimen

Similar to the plate specimen, an experiment was completed in order to further investigate the results concluded by the finite element model for the connection specimen. A connection system was constructed, shown previously as Figure 7a and tested. Each of the bases for the specimen was supported by a rubber pad. Two tri-axial accelerometers and one uniaxial accelerometer were placed on the specimen and an impact hammer was used to input an impulse force in the x-direction. The layout of this experiment is shown in Figure 9. Acceleration data was gathered for all sensors for each of seven damage severities (0, 1, 2, 3, 4, 5, and 6 bolts removed). The damage was

introduced by successively removing one bolt from the connection of interest. The pattern of bolt removal is shown in Figures 9b and 9c.

Using the data acquisition software DeweSoft (DeweSoft 2011), real-time calculations were computed to determine the coherence of the signals between the reference node and each of the response nodes for all damage scenarios. The coherence is a statistical process in which to measure the linearity relationship between the input and output signals in a linear system. The coherence values are ranging between 0 and 1. A coherence of 1 indicated a purely linear relationship while a coherence of 0 indicated no relationship between the signals. Other values between 0 and 1 indicated the noise and nolinearity of the system. Coherence is calculated by using Equation 11, where G_{xy} is the cross-spectral density between the input signal x and the output signal y, and G_{xx} and G_{yy} are the auto-spectral densities for signals x and y, respectively. The values obtained by this calculation are used to determine ranges in frequency in which noise or nonlinearity occurs between the signals.

$$C_{xy} = \frac{|G_{xy}|^2}{G_{xx}G_{yy}} \tag{11}$$

The calculated coherence for each of the damage scenarios is shown in Figure 10. Upon inspection, the coherence is high (> 0.9) for most of the signal between nodes 2 and 3 for all damage scenarios, while the range of high coherence between nodes 2 and 1 is limited to between 20 to 45 and 62 to 72. This suggests that nonlinearity is introduced into the system between nodes 2 and 3 at the frequency ranges corresponding to low coherence.
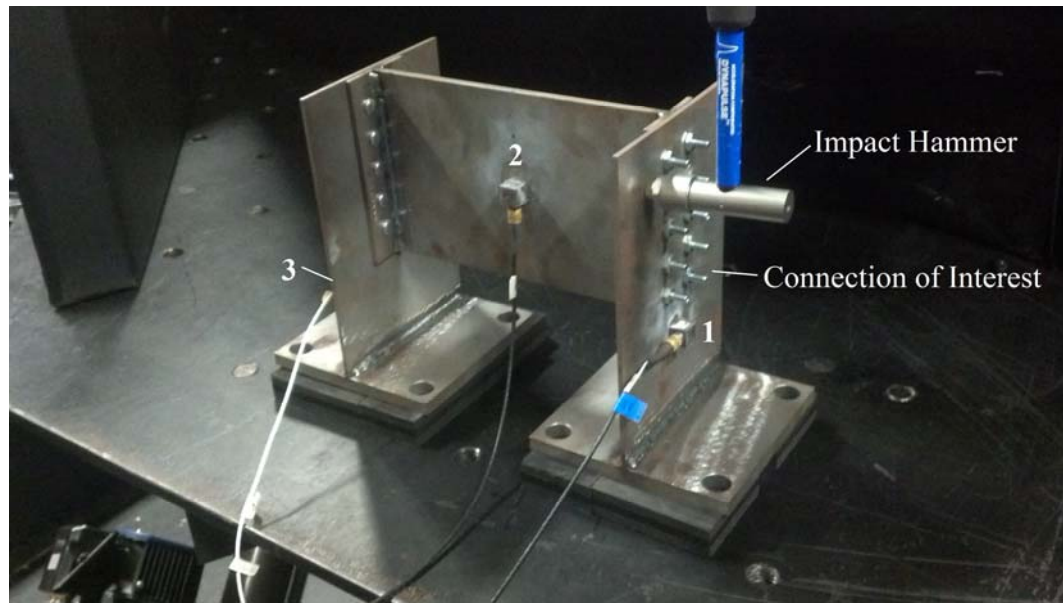
(a)
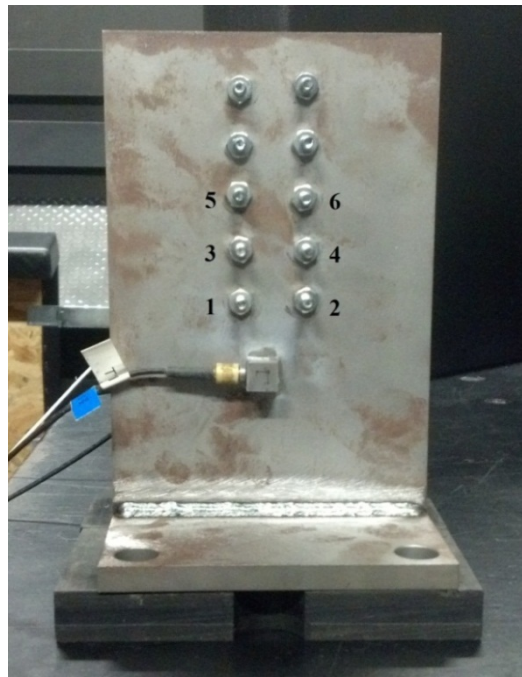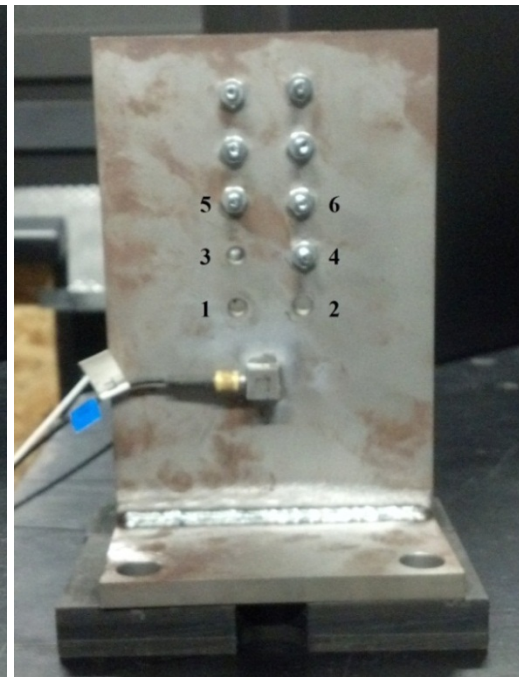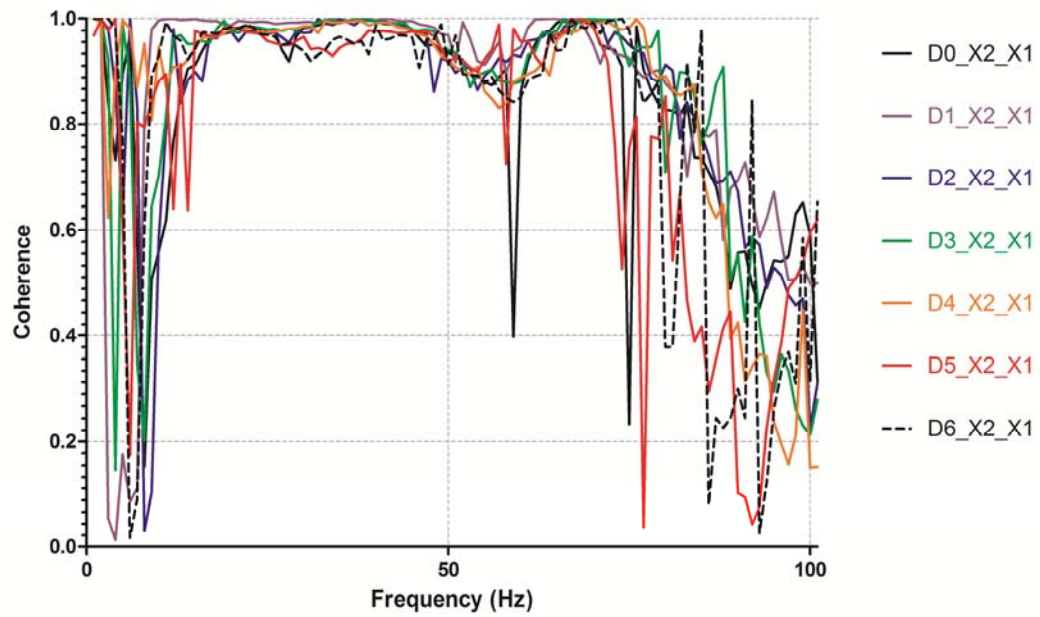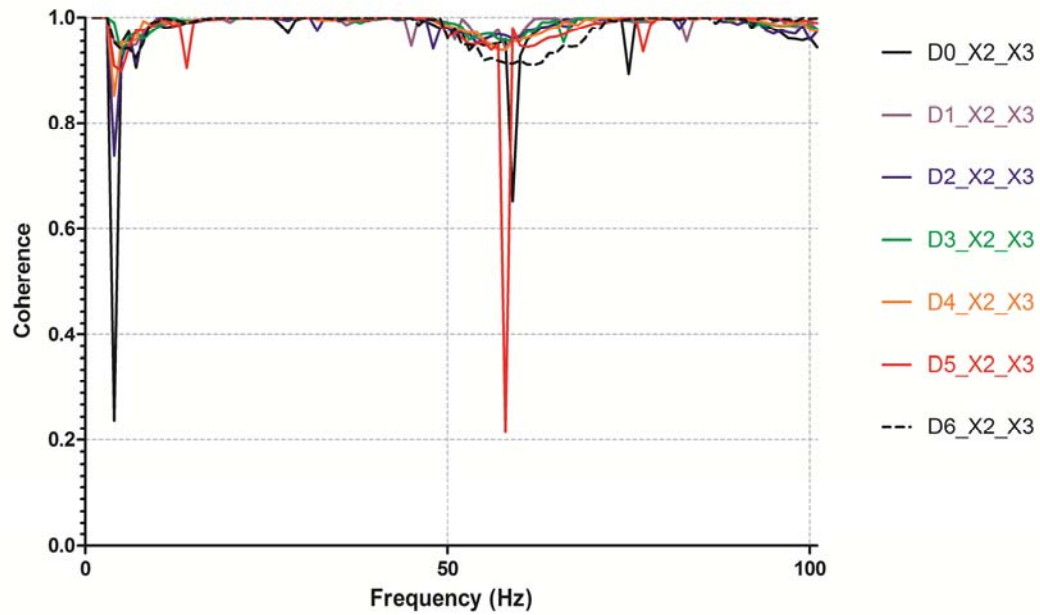

(b)   (c)

Figure 9. Experimental layout of connection specimen (a) Placement of nodes and
location of impact (b) Connection specimen bolt removal plan showing
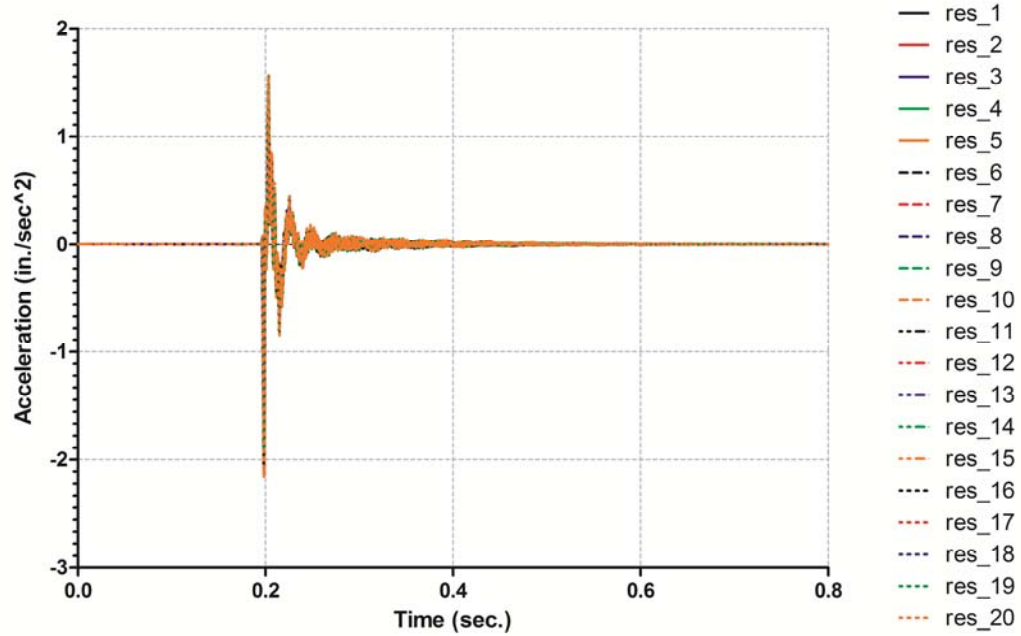damage scenario D0 (c) Damage scenario D3

(a)

(b)

Figure 10. Coherence of signals for experimental connection specimen (a) Signals between Nodes 2 and 1 (b) Signals between Nodes 2 and 3

To further investigate the linearity captured by the coherence, the data acquired for this experiment was then used to calculate the FRF for the connection specimen. The notation for each damage scenario is D#_Ref_Res, where # is the number of bolts removed from the connection, Ref refers to the reference node, and Res refers to the response node. For example, D3_2_1 corresponds to the damage scenario with 3 bolts removed from the connection, with node 2 as the reference signal and node 1 as the response signal. The acceleration signal of the X direction for node 1 for each of the 20 impacts when zero bolts were removed is shown in Figure 11a. The FRFs of nodes 1 and 2 for each of these 20 impacts when zero bolts were removed is shown in Figure 11b. The averaged FRF for each damage scenario is shown in Figure 12.

<u>Connection Specimen Results and Discussion</u>

Similar to the trend from the plate specimen, damage can be found, quantified and located for the connection specimen. Figure 12a shows that there is damage between nodes 1 and 2 by the decrease in the magnitude of the FRF over the range of frequencies with high coherence. This damage can be quantified by the trend the response follows for each damage scenario. It is noted that the accuracy of the quantification is related to the supervised learning process in which the data was gathered. To append to an unsupervised learning process, this damage could be quantified by categorizing the damage trend into healthy, light damage, moderate damage, or severe damage based on the amount of change from the initial data set. Figure 12b shows that the response of the specimen acts very similar between nodes 2 and 3 for each damage scenario. This, along with the high coherence between these signals, suggests that there is no impairment between these nodes. The strong correlation between signals can also be seen by Figure

11a. This correlation can be extended throughout the calculations as shown by the strong correlation between the FRFs in Figure 11b. When directly comparing the relationships between each pair of nodes, as shown in Figure 12c, it is clear that a change is occurring between nodes 2 and 1 by the variation in response to damage. By looking only at regions of linearity, i.e. looking at regions of high coherence, it is shown that a trend appears in which damage decreases the frequency response of the system only between the nodes that the damage is located. The frequency ranges looked at are 17-50 Hz and 65-72 Hz.
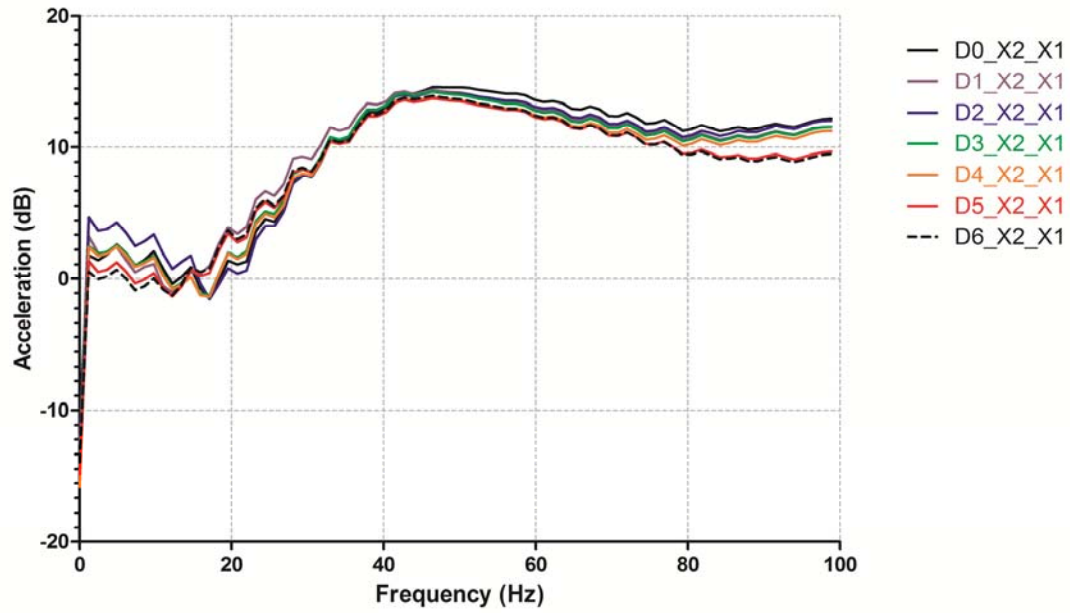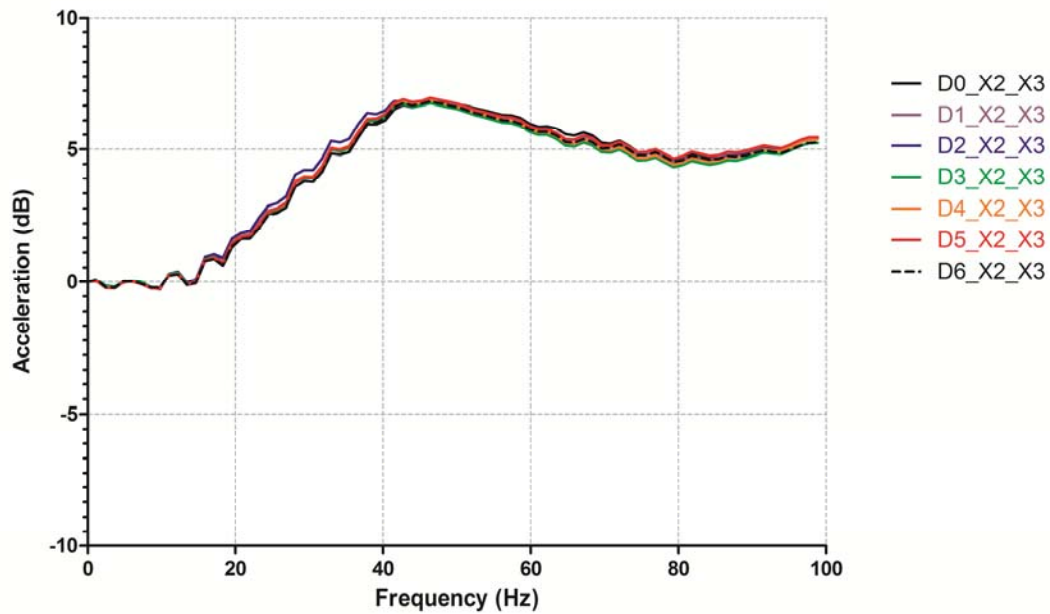
(a)
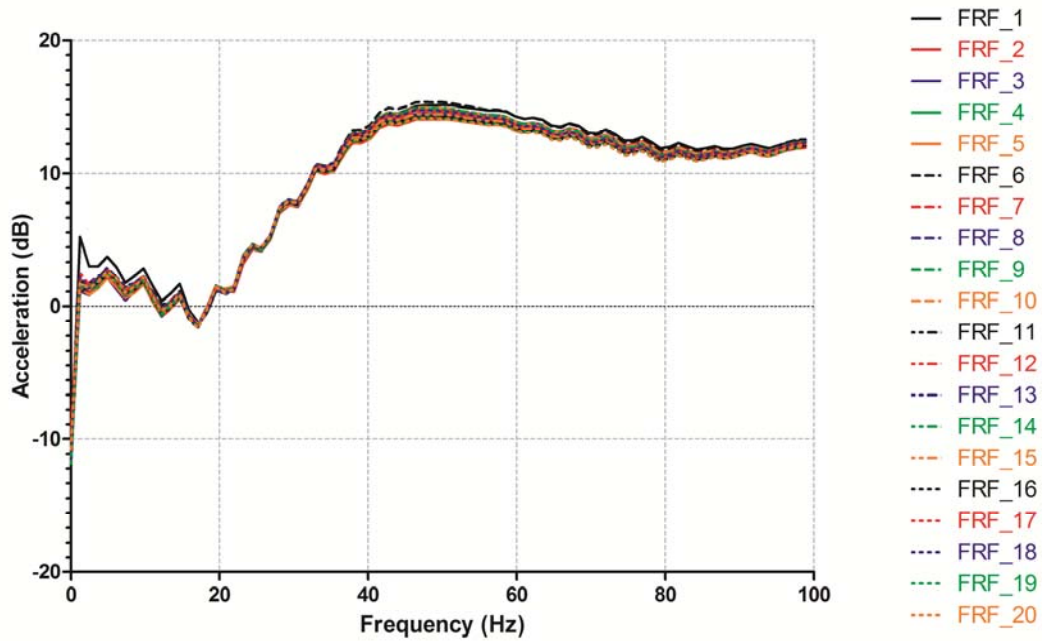
(b)

Figure 11. Data for 20 impacts on connection specimen for D0 (a) Acceleration Signals at X1 (b) FRF of X1 and X2

(a)

(b)

Figure 12. FRF diagrams of experimental connection specimen (a) Multiple damage scenarios at Nodes 2 and 1 (b) Multiple damage scenarios at Nodes 2 and 3 (c) Comparison of relationships between responses of each pair of nodes
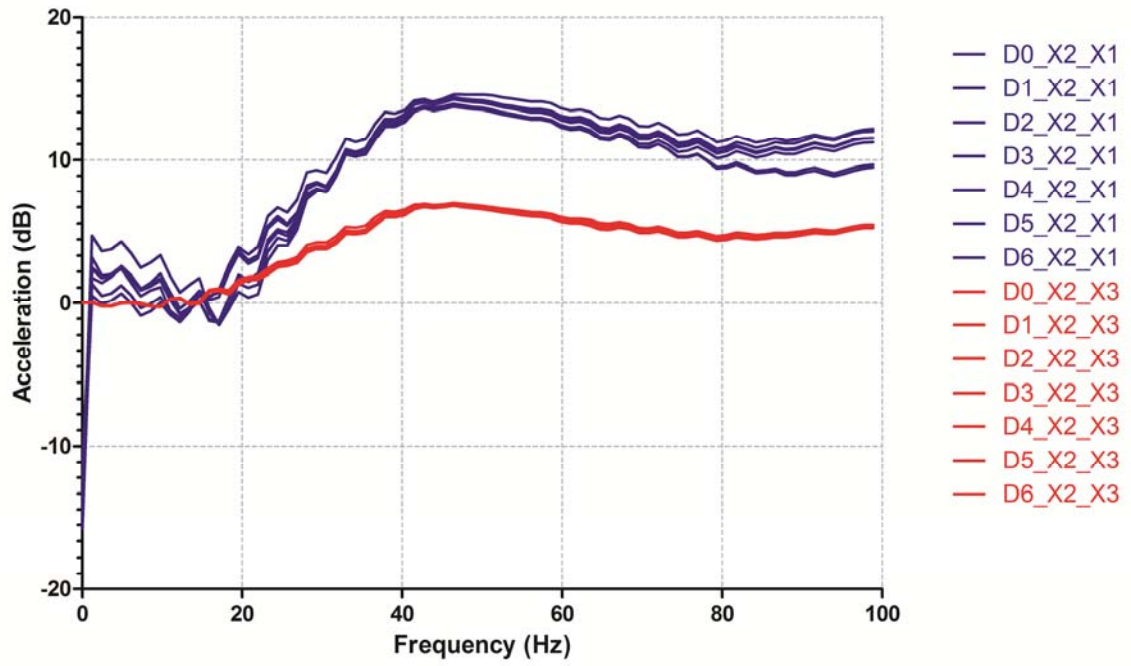
Figure 12. Continued

CONCLUSION

Based on the work conducted, it can be concluded that by localizing dynamic response sensors, damage could be detected, quantified and located for varying damage severities and for different geometrically constrained systems. Numerical calculation was used to provide insight into the investigation as well as accurately prove the experimental analyses. Although the finite element model for the plate specimen yielded slightly tighter FRF results from that seen by the experimental results for the plate specimen, it is concluded that damage could be detected in both analyses by the trend of decreasing magnitude of the response function for increasing damage. It can also be concluded that both models could be completed using non-destructive, unsupervised learning processes based on the expected changes in the FRF, therefore could be utilized in real-world situations in which damage detection is needed.

Future exploration with this method would include application with bridge monitoring under normal traffic loading. A preliminary analysis has been conducted for this scenario, using data collected for a thirty minute time period. Three sensors were located across a floor beam in the middle span of a three-span highway bridge, with two sensors attached to the web of each girder near the connection of the girder and floor beam, and the third sensor attached to the web of the floor beam at mid-span. The algorithm presented was utilized for this data, and the preliminary results show that the method is promising, but requires further investigation due to the complexity of the loading and the complexity of the deformation of the bridge itself. The loading is complex due to the variability in vehicle size and weight, as well as the multiple traffic lanes, and the impact between the vehicle and the bridge (at the abutment locations)

which also causes the vehicle to oscillate when traveling over the bridge. The deformation of the bridge is complex due to the combination of in-plane and out-of-plane bending and torsion on the girders and substructure. Further investigation would focus on, but is not limited to, collecting consistent data, determining the effect of the vehicular oscillation on the bridge response, and refining the filtering process such that consistent data can become cleaner for the analysis.

BIBLIOGRAPHY

Adewuyi, A. P., Z. Wu, et al. 2009. "Assessment of vibration-based damage identification methods using displacement and distributed strain measurements." Structural Health Monitoring, 8(6): 443-461.

ANSYS (Release 13.0) [Software]. (2010). ANSYS, Inc.

Chang, P. C., A. Flatau, et al. 2003. "Review Paper: Health monitoring of civil infrastructure." Structure Health Monitoring, 2(3): 257-267.

Chase, S. B. (2001). "Smarter bridges, why and how?" Smart Materials Bulletin, 9-13.

Cruz, Paulo J. S., and Rolando Salgado. 2008. "Performance of Vibration-Based Damage Detection Methods in Bridges." Computer-Aided Civil and Infrastructure Engineering, 24: 62-79.

DeweSoft (Version 7.0.5 b14) [Software]. (2011). DeweSoft.

Duffey, T. A., S. W. Doebling, et al. 2001. "Vibration-based damage identification in structures exhibiting axial and torsional response." Transaction of the ASME, 123: 84-91.

Farrar, C. R. and D. A. Jauregui 1998. "Comparative study of damage identification algorithms applied to a bridge: I. Experiment." Smart Materials and Structures, 7: 704-719.

Fugate, Michael L., Hoon Sohn, and Charles R. Farrar. 2000. "Unsupervised Learning Methods for Vibration-Based Damage Detection" 18th IMAC, San Antonio, Texas.

Hou, Z., M. Noori, and R. St. Amand. 2000. "Wavelet-Based Approach for Structural Damage Detection" Journal of Engineering Mechanics, 126 (7).

Humar, J., A. Bagchi, et al. 2006. "Performance of vibration-based techniques for the identification of structural damage" Structural Health Monitoring, 5(3): 215-241.

Li, S. and Z. Wu. 2007. "Development of distributed Long-gage fiber optic sensing system for structural health monitoring." Structural Health Monitoring, 6(2): 133-143.

Li, S. Z. and Z. S. Wu. 2007. "A non-baseline algorithm for damage locating in flexural structures using dynamic distributed macro-strain responses." Earthquake Engineering and Structural Dynamics, 36: 1109-1125.

Law, S. S., X. Y. Li, X. Q. Zhu, and S. L. Chen. 2005. "Structural damage detection from wavelet packet sensitivity" Engineering Structures, 27.

Maia, N. M. M., J. M. M. Silva, et al. 2003. "Damage detection in structures: from mode shape to frequency response function methods" Mechanical Systems and Signal Processing, 17(3): 489-498.

Pandey, A. K., M. Biswas, et al. 1991. "Damage detection from changes in curvature mode shapes." Journal of Sound and Vibration, 145: 312-332.

Peeters, Bart, Johan Maeck and Guido De Roeck. 2001. "Vibration-based damage detection in civil engineering: excitation sources and temperature effects" Smart Materials and Structures, 10.

Rytter, A. 1993. "Vibration based inspection of civil engineering structures." PhD Dissertation, Department of building Technology and Structural Engineering, Aalborg University, Denmark.

Sampaio, R. P. C., N. M. M. Maia, et al. 1999. "Damage detection using the frequency-response function curvature method." Journal of Sound and Vibration, 226(5): 1029-1042.

Wahab, M. M. A. and G. D. Roeck. 1999. "Damage detection in bridges using modal curvatures: application to a real damage scenario." Journal of Sound and Vibration, 226(2): 217-235.

Yang, J. N., Y. Lei, S. Lin, and N. Huang. 2004. "Hilbert-Huang Based Approach for Structural Damage Detection" Journal of Engineering Mechanics, 130 (1).